Orientation and Dynamics of Chainlike Dipole Arrays: Donor−Acceptor-Substituted Oligophenylenevinylenes in a Polymer Matrix

C. Former, H. Wagner, R. Richert,*,† D. Neher,‡ and K. Müllen

Max-Planck-Institut für Polymerforschung, Ackermannweg 10, 55128 Mainz, Germany

Received February 19, 1999; Revised Manuscript Received October 8, 1999

ABSTRACT: We have investigated the orientational behavior of a series of novel oligophenylenevinylenes which carry a sequence of hyperpolarizable and dipolar donor−acceptor (DA) pairs, designed to allow for a free rotation of the DA orientation in a plane perpendicular to the long molecular axis. The studies include both the measurement of effective dipole moments, which are relevant for the degree of polar ordering required for second-harmonic generation, and the assessment of the time scales involved in the orientational motion of the effective dipole moment. The comparison between calculated dipole moments and those measured for different oligomers in toluene solution and in a polystyrene matrix confirm that a DA-pair separation of ≈10 Å along the oligomer leads to a high chromophore concentration in the sample, yet without the unfavorable effect of aggregation or antiparallel alignment of neighboring dipole pairs. Both the bulkiness of the oligomer molecules and the electrostatic coupling of adjacent dipoles give rise to an improved stability of the field-induced chromophore alignment. In contrast to the monomeric stilbene-like model compounds, the time scale of oligomer reorientation parallels the structural relaxation time of the polymeric host material.

1. Introduction

Poled polymers are widely investigated as regards their potential as nonlinear optical devices.[1−8] They usually consist of dye molecules embedded at low concentrations, $c \ll 1$, in the bulk polymer matrix. The particular dyes are selected so as to exhibit large values for the hyperpolarizability, β, combined with large permanent dipole moments, μ.[1−4] The efficiency of such a device, e.g., for second-harmonic-generation (SHG), depends on c and β and indirectly on μ, because the dipole moment is an important factor in determining the average orientation $\langle\cos\theta\rangle$ of the dye molecules which can be achieved with a certain poling field.[9] The situation of aligned chromophores, $\langle\cos\theta\rangle \neq 0$, breaks the centrosymmetry of the sample as required for obtaining second-order nonlinear optical properties of the macroscopic sample.[2−4]

In such systems, field poling is done at temperatures at which the matrix is sufficiently mobile, i.e., above the glass transition temperature T_g. The sample is then cooled to below T_g in order to suppress orientational degrees of freedom which would tend to randomize the molecular orientations thereby restoring the centrosymmetry.[9,10] In particular, for dissolved dye molecules (opposed to those which are attached to or incorporated in the polymer main chain), it is often observed that the long-term stability as regards $\langle\cos\theta\rangle$ remains insufficient for practical applications.[7,8,11] A further drawback of dissolved standard dyes, e.g., disperse red (DR1) or dimethylaminonitrostilbene (DANS), is their tendency to form aggregates at concentrations in excess of $c \approx 1\%$, in which antiparallel configurations are preferred due to the electrostatic interactions of strong dipoles.

The inevitable tendency for thermal randomization of an aligned ensemble of dopants after the removal of the dc-poling field has been the subject of intense research.[5−8,11−16] The associated decay of an SHG intensity reflects the temporal stability of the macroscopic second-order susceptibility $\chi^{(2)}$, which depends mainly on the orientation of the chromophores. An important issue in this context is the coupling of the dopant's reorientation to the structural or α-relaxation of the host matrix. Dielectric measurements[3,13,17] and thermally stimulated discharge experiments (TSD)[11,15] have been employed extensively in order to characterize the ensemble-averaged orientational dynamics of such guest/host materials and to compare the results with the SHG decay patterns. In the case of a low guest concentration in a polar host, such dielectric relaxation measurements reflect the bulk behavior rather than selectively probing the alignment of guest molecules. That the dynamics of guest and host molecules can differ significantly has been demonstrated in various experimental studies.[18] Therefore, an independent measure of the chromophore reorientation is usually lacking, although required for assessing all factors which can affect the SHG intensity other than the guest alignment.[19,20] Furthermore, the motional degrees of freedom and mutual interactions are crucial parameters in a situation where several chromophores are incorporated in a single molecule.

The present concept is to investigate a homologous series of chromophores, in which various properties can be taylored independently. To this end, we employ a previous method of ours for synthesizing phenylenevinylenes[21−24] with the following capabilities: (i) incorporation of strong dipoles at the double-bond; (ii) variation of the number of dipoles per oligomer; (iii) variation of the dipole−dipole separation; (iv) arbitrary dipole sequence along the π-conjugated chain; (v) alteration of the bulkiness of lateral substituents (methyl or butyl); (vi) formation of the analogous polymers.

†Permanent address: Department of Chemistry and Biochemistry, Arizona State University, Tempe, AZ 85287-1604.

‡Permanent address: Institut für Physik, Universität Potsdam, 14415 Potsdam, Germany.

10.1021/ma9902403 CCC: $18.00
Published on Web 11/13/1999

Scheme 1. Donor- and Acceptor-Substituted Oligomers, 1a,b, 2a,b, 3a,b, and Polymer 4b, Which Represent π-conjugated Chains, Where the Oligomers Carry Respectively $N = 1$, 2, or 3, Dipoles Per Molecule, Whereas the Polymeric Analogue Has 2n Dipoles Per n Repeat Units

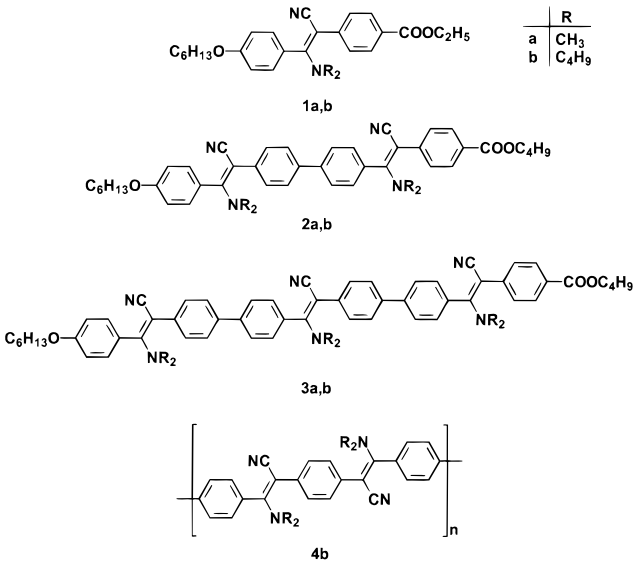

The crucial step of the synthesis is the double bond formation by a simple cation−anion coupling. Treating benzyl cyanide derivatives with sodium hydride in DMF at −60 °C leads to the corresponding anions which can be coupled with ammonium salts to give phenylenevinylenes, which contain amino and nitrile substituents at the vinylene position. We assume that there is no other method to synthesize phenylenevinylenes with strong dipoles at the vinylene position in such an elegant way and in nearly quantitative yields. Eventually, we were able to synthesize **1a**,**b**, **2a**,**b**, and **3a**,**b** shown in Scheme 1, which represent a homologous series of oligophenylenevinylenes with cyano and dimethylamino (**1a**, **2a**, **3a**) or dibutylamino (**1b**, **2b**, **3b**) substituents. On the basis of the high yield of the reaction, we also achieved the synthesis of polymer **4b**, which is quite soluble in common polar solvents and excellently processable into clear films.[21]

In contrast to unsubstituted stilbenes and poly(*p*-phenylenevinylenes), which represent planar systems with conjugated double bonds, our oligophenylenevinylenes are predominantly flexible molecules wherein the dipoles are assumed to rotate almost freely in a plane perpendicular to the long molecular axis. The reason for this degree of freedom is the donor and acceptor strength of the substituents which leads to an intramolecular charge transfer. As a result, the molecule segments are not only able to rotate around σ-bonds (conformational mobility) but also are able to rotate around the double bond, which possesses single bond character (configurational mobility) as indicated in Scheme 2.[22] According to ^{1}H NMR studies of donor- and acceptor-substituted stilbenes, the equilibrium ratio between the cis and trans isomers is 43:57.

Within the homologous series of molecules compiled in Scheme 1, we anticipate that also the physical properties are varied in a systematic manner. The effect of dipole separation can be addressed by comparing the current findings with results obtained previously for analogous oligomers with phenyl or tolan spacers between the chromophores. This variation of the dipole

Scheme 2. Intramolecular Charge Transfer Leading to Phenylenevinylenes with Conformational and Configurational Mobility (in the Present Schemes Only the Trans Isomers Are Shown)

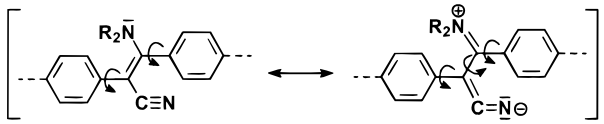

Scheme 3. Synthesis of 4-(cyanomethyl)Benzoic Acid Alkyl Esters 6a and 6b, Used as Nucleophilic Compounds in the Oligomer Syntheses

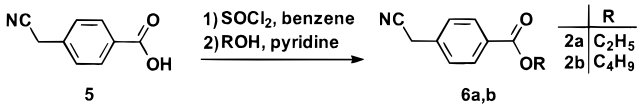

Scheme 4. Synthesis of the Ammonium Salts 10a and 10b, Used as Electrophilic Compounds in the Oligomer Syntheses

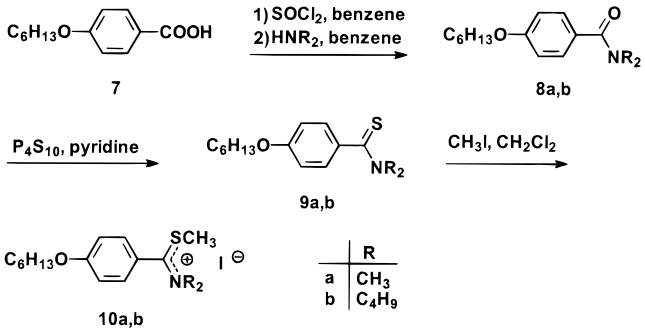

distances d is important for assessing the role of electrostatic interactions. Such interactions of neighboring dipoles will frustrate their ability to rotate independently and eventually lead to the unfavorable case of antiparallel orientations, for which no polar order can be established.

The aim of our systematic study is to explore the possibilities of enhancing the chromophore concentration by gathering dipoles in a molecule, without affecting the high degree of polar order. Using dielectric techniques, we investigate the effective dipole moments and the orientational dynamics of these molecules dissolved at a concentration of $c = 5\%$ in the nonpolar matrix polystyrene. In these materials, the dielectric relaxation originates from the dynamics of the guest molecules only. The orientational behavior of the dipolar groups is discussed as a function of the number of repeat units, the dipole separation within the oligomer, and the bulkiness of alkyl side groups. The dynamical features are compared with those of bulk polystyrene in order to assess the dynamical coupling of these guest molecules to the matrix. The effective dipole moments of the oligomers measured in toluene and polystyrene as a function of the number of repeat units allows one to quantify the rotational degrees of freedom as well as the importance of dipole−dipole interactions within a molecule.

2. Experimental Section

2.1. Synthesis of Compounds. In this section we describe the synthesis of the starting materials **6a**,**b** (Scheme 3) and **10a**,**b** (Scheme 4) and the oligomers **1a**,**b** (Scheme 5), **2a**,**b**, and **3a**,**b** (Scheme 6). The synthesis of polymer **4b** has been described previously.[21] NMR spectra were recorded using a Bruker AC 300 spectrometer. Chemical shifts are given on the

Scheme 5. Condensation of 6a and 10a,b for the Synthesis of Stilbenes 1a and 1b

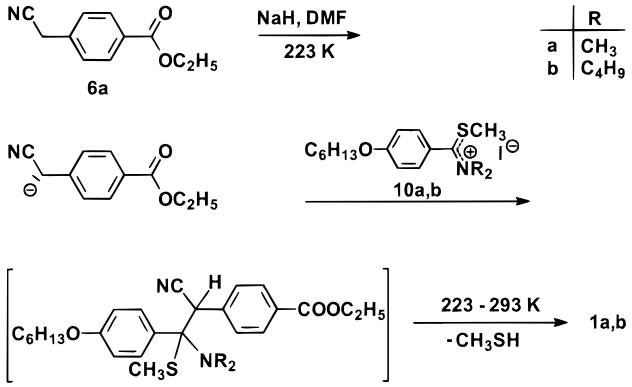

Scheme 6. Synthesis of Oligomers 2a,b and 3a,b via a One-pot Successive Buildup

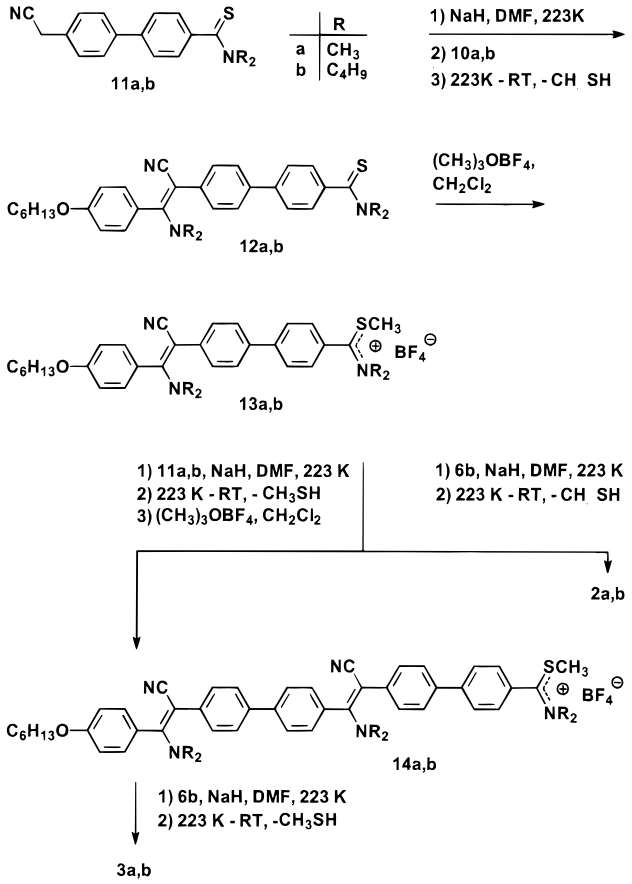

δ scale in parts per million relative to tetramethylsilane as internal standard. Calibration of the ^{1}H and ^{13}C NMR spectra was carried out by means of solvent peaks (for $CDCl_3$): $\delta(^1H) = 7.24$; $\delta(^{13}C) = 77.0$. IR spectra were obtained using a Nicolet 320 FT-IR spectrometer. UV−vis spectra were recorded using a Perkin-Elmer Lambda 15. Mass spectrometry was performed using a VG ZAB 2-SE-FPD by means of field desorption (FD).

2.1.1. 4-(Cyanomethyl)benzoic acid Ethyl Ester (6a). (For the general procedure, see Scheme 3.) 4-(Cyanomethyl)-benzoic acid (**5**)[25] (11.31 g, 70.25 mmol) was dissolved in benzene (150 mL), and DMF (1 mL) and thionyl chloride (50 mL, 700 mmol) were added. The solution was heated at reflux for 24 h, and after the reaction was allowed to cool, the solvent and remaining thionyl chloride were distilled off under vacuum. The residue was dissolved in benzene (200 mL), pyridine (200 mL), and ethanol (24.7 mL, 420 mmol). After this solution was heated at reflux for 24 h, the solvent was removed under vacuum and the residue was fractionally distilled (353 K, 0.08 mbar). Yield: 13.3 g (79%). ^{1}H NMR ($CDCl_3$, 300 MHz), δ: 8.08, 7.44 (2 × d, 4H, ArH), 4.40 (m, 2H, $-CH_2CH_3$), 3.81 (s, 2H, CH_2CN), 1.43 (t, 3H, CH_3). ^{13}C NMR ($CDCl_3$, 75 MHz), δ: 165.8, 134.6, 130.1, 129.7, 127.7, 117.1, 61.2, 23.3, 14.0, 0.8. IR [cm^{-1}], ν: 2983, 2359, 2341, 2254, 1715, 1614, 1368, 1109, 967, 733. Anal. Calcd for $C_{11}H_{11}NO_2$ (189.2): C, 69.83; H, 5.86; N, 7.40. Found: C, 69.70; H, 5.81; N, 7.26.

2.1.2. 4-(Cyanomethyl)benzoic acid Butyl Ester (6b). 4-(Cyanomethyl)benzoic acid butyl ester (**6b**) was prepared from 4-(cyanomethyl)benzoic acid (**5**) (10.00 g, 62.11 mmol), thionyl chloride (45 mL, 620 mmol), and butanol (34.0 mL, 370 mmol) in the manner described in the general procedure. Purification has been achieved by column chromatography with an eluent mixture of petroleum ether/ethyl acetate 3:1. Yield: 5.4 g (40%). ^{1}H NMR ($CDCl_3$, 300 MHz), δ: 8.05, 7.40 (2 × d, 4H, ArH), 4.33 (t, 2H, $-OCH_2$), 3.80 (s, 2H, CH_2CN), 1.73 (m, 2H, $-OCH_2-CH_2$), 1.47 (m, 2H, $-OCH_2-CH_2-CH_2$), 0.98 (t, 3H, CH_3). ^{13}C NMR ($CDCl_3$, 75 MHz), δ: 165.9, 134.6, 130.3, 127.8, 117.1, 65.0, 30.6, 25.5, 23.5, 19.1, 13.7. IR [cm^{-1}], ν: 2961, 2934, 2359, 2253, 1716, 1615, 1282, 1111, 907, 732. MS (FD, 8kV), m/z: 217.2 (M^+). Anal. Calcd for $C_{13}H_{15}NO_2$ (217.3): C, 71.87; H, 6.96; N, 6.44. Found: C, 71.70; H, 6.87; N, 6.40.

2.1.3. 4-Hexyloxy-*N*,*N*-dibutylbenzamide (8b). (For the general procedure, see Scheme 4.) Thionyl chloride (69.6 g, 0.585 mol) was added to a solution of 4-hexyloxybenzoic acid (**7**)[26] (26 g, 0.117 mol) and benzene (500 mL) and heated at reflux. After a reaction time of 10 h, the solvent and remaining thionyl chloride were removed under vacuum. Benzene (600 mL) was added and the mixture cooled to 280 K. *N*,*N*-Dibutylamine (45.4 g, 0.351 mol) was added dropwise, and the reaction solution was stirred for 10 h at room temperature. After addition of water (300 mL) and stirring for another hour the organic phase was separated and washed with 300 mL of 2 N acetic acid. The solvent was distilled under vacuum and 4-hexyloxy-*N*,*N*-dibutylbenzamide (**8b**) was obtained in 92% yield (35.9 g).

^{1}H NMR ($CDCl_3$, 300 MHz), δ: 7.30, 6.87 (2 × d, 4H, ArH), 3.97 (t, 2H, $-OCH_2$), 3.34 (m, 4H, NCH_2), 1.82−0.88 (m, 25H, $N(CH_2-C_3H_7)_2$, $OCH_2-C_5H_{11}$). ^{13}C NMR ($CDCl_3$, 75 MHz), δ: 170.9, 137.9, 136.1, 135.2, 134.6, 49.4, 48.7, 44.4, 32.4, 32.0, 30.4, 30.8, 29.5, 26.3, 23.0, 20.2, 19.6, 14.4, 13.8, 13.5. MS (FD, 8kV), m/z: 333.1 (M^+), Anal. Calcd for $C_{21}H_{35}NO_2$ (333.5): C, 75.63; H, 10.58; N, 4.20. Found: C, 75.60; H, 10.61; N, 4.16.

2.1.4. 4-Hexyloxy-*N*,*N*-dimethylbenzamide (8a). 4-Hexyloxy-*N*,*N*-dimethylbenzamide (**8a**) was prepared from 4-hexyloxybenzoic acid (**7**)[26] (10.0 g, 0.045 mol), thionyl chloride (26.8 g, 0.225 mol), and *N*,*N*-dimethylamine (6.75 g, 0.150 mol). Yield: 10.55 g (94%). ^{1}H NMR ($CDCl_3$, 300 MHz), δ: 7.38, 6.88 (2 × d, 4H, ArH), 3.98 (t, 2H, $-OCH_2$), 3.05 (2 × s, 6H, NCH_3), 1.77 (m, 2H, OCH_2-CH_2), 1.49−1.27 (m, 6H, $C_3H_6-CH_3$), 0.92 (t, 3H, CH_3). ^{13}C NMR ($CDCl_3$, 75 MHz), δ: 171.2, 137.9, 136.3, 128.5, 126.8, 49.1, 38.1, 35.2, 32.4, 30.6, 26.3, 23.1, 14.5. MS (FD, 8kV), m/z: 249.1 (M^+). Anal. Calcd for $C_{15}H_{23}NO_2$ (249.3): C, 72.25; H, 9.30; N, 5.61. Found: C, 72.10; H, 9.21; N, 5.58.

2.1.5. 4-Hexyloxy-*N*,*N*-dibutylthiobenzamide (9b). (For the general procedure, see Scheme 4.) 4-Hexyloxy-*N*,*N*-dibutylbenzamide (**8b**) (35.9 g, 0.108 mol) was dissolved in pyridine (300 mL), and phosphorus(V) sulfide (0.026 mol, 11.5 g) was added. The solution was heated at reflux for 24 h, the solvent was removed under vacuum, and the residue was purified by column chromatography with an eluent mixture of petroleum ether/ethyl acetate 1:1.

Yield: 26.42 g (70%). ^{1}H NMR ($CDCl_3$, 300 MHz), δ: 7.16, 6.82 (2 × d, 4H, ArH), 4.05, 3.43 (2 × t, 4H, NCH_2) 3.96 (t, 2H, $-OCH_2$), 1.90−0.75 (m, 25H, $N(CH_2-C_3H_7)_2$, $OCH_2-C_5H_{11}$). ^{13}C NMR ($CDCl_3$, 75 MHz), δ: 200.1, 143.6, 142.4, 139.2, 138.1, 52.3, 50.4, 49.4, 32.6, 32.1, 29.5, 27.0, 26.5, 23.1, 19.2, 18.7, 14.5, 12.5. MS (FD, 8kV), m/z: 349.1 (M^+). Anal. Calcd for $C_{21}H_{35}NOS$ (349.5): C, 72.15; H, 10.09; N, 4.00. Found: C, 71.98; H, 10.05; N, 3.97.

2.1.6. 4-Hexyloxy-*N*,*N*-dimethylthiobenzamide (9a). 4-Hexyloxy-*N*,*N*-dimethylthiobenzamide (**9a**) was prepared from 4-hexyloxy-*N*,*N*-dimethylbenzamide (**8a**) (20.00 g, 0.080

mmol) and phosphorus(V) sulfide (8.58 g, 0.019 mol) in the manner described in the general procedure. Yield: 14.44 g (68%). ^{1}H NMR ($CDCl_3$, 300 MHz), δ: 7.27, 6.84 (2 × d, 4H, ArH), 3.96 (t, 2H, $-OCH_2$), 3.58, 3.20 (2 × s, 6H, NCH_3), 1.78 (m, 2H, OCH_2-CH_2), 1.45−1.31 (m, 6H, $C_3H_6-CH_3$), 0.91 (t, 3H, CH_3). ^{13}C NMR ($CDCl_3$, 75 MHz), δ: 199.6, 143.0, 142.0, 138.8, 135.8, 49.7, 44.4, 42.2, 32.4, 30.5, 26.5, 23.1, 14.3. MS (FD, 8kV), *m*/*z*: 265.1 (M^+). Anal. Calcd for $C_{15}H_{23}NOS$ (265.3): C, 67.88; H, 8.73; N, 7.40. Found: C, 68.72; H, 8.79; N, 7.40.

2.1.7. 4-Hexyloxydibutyl[(methylthio)phenylmethylene]-ammonium Iodide (10b). (For the general procedure, see Scheme 4.) 4-Hexyloxy-*N*,*N*-dibutylthiobenzamide (**9b**) (5.00 g, 14.3 mmol) was dissolved in dichloromethane (50 mL) under an argon atmosphere. After addition of methyl iodide (6.09 g, 42.9 mmol) the solution was stirred for 48 h at room temperature. The solvent and remaining methyl iodide were removed under vacuum, and **9b** was obtained in 97% yield (7.02 g) after purification by chromatography on silica gel with acetonitrile.

^{1}H NMR ($CDCl_3$, 300 MHz), δ: 7.08, 6.63 (2 × d, 4H, ArH), 4.13, 3.77 (2 × t, 4H, NCH_2) 4.01 (t, 2H, $-OCH_2$), 2.31 (s, 3H, SCH_3), 1.91−0.73 (m, 25H, $N(CH_2-C_3H_7)_2$, $OCH_2-C_5H_{11}$). ^{13}C NMR ($CDCl_3$, 75 MHz), δ: 191.3, 128.5, 120.3, 115.4, 113.4, 67.7, 57.8, 55.7, 47.4, 30.8, 30.3, 29.7, 28.3, 27.5, 24.9. 21.8, 19.5, 18.9, 13.3, 12.8. IR[cm^{-1}] ν: 2961, 2934, 2874, 2252, 2200, 1709, 1604, 1507, 1257, 910, 733. MS (FD, 8kV), *m*/*z*: 364.5 ($M^+ - 127(I^-)$).

2.1.8. 4-Hexyloxydimethyl[(methylthio)phenylmethylene]ammonium Iodide (10a). 4-Hexyloxydimethyl[(methylthio)phenylmethylene]ammonium iodide (**10a**) was prepared from 4-hexyloxy-*N*,*N*-dimethylthiobenzamide (**9a**) (5.00 g, 0.019 mol) and methyl iodide (8.09 g, 0.057 mol) in the manner described in the general procedure. Yield: 92% (7.12 g). ^{1}H NMR ($CDCl_3$, 300 MHz), δ: 7.40, 7.09 (2 × d, 4H, ArH), 4.04 (t, 2H, $-OCH_2$), 3.75, 3.46 (2 × s, 6H, NCH_3) 2.25 (s, 3H, SCH_3), 1.80 (m, 2H, OCH_2-CH_2), 1.47−1.32 (m, 6H, $-C_3H_6-CH_3$), 0.91 (t, 3H, CH_3). ^{13}C NMR ($CDCl_3$, 75 MHz), δ: 191.0, 161.9, 129.0, 121.1, 115.6, 68.2, 47.1, 44.5, 31.2, 28.7, 25.4, 22.3, 18.2, 13.8, 11.3, IR [cm^{-1}], ν: 2932, 2872, 2860, 2253, 1694, 1509, 1256, 1179, 1963, 906, 745. MS (FD, 8kV), *m*/*z*: 280.1 ($M^+ - 127(I^-)$).

2.1.9. Stilbene 1a. (For the general procedure, see Scheme 5.) 4-(Cyanomethyl)benzoic acid ethyl ester (**6a**) (500 mg, 2.64 mmol) and DMF (4 mL) were cooled to 233 K, after which sodium hydride (95% w/w dispersion in mineral oil) (133 mg, 5.28 mmol) and 4-hexyloxydimethyl[(methylthio)phenylmethylene]ammonium iodide (**10a**) (1.075 g, 2.64 mmol) were added. After 6 h, the solution was warmed to room temperature. The solvent was removed under vacuum, and the residue was purified by chromatography on silica gel with an eluent mixture of ethyl acetate/petroleum ether 1:5. The glassy, yellow product **1a** was obtained in 28% total yield (314 mg).

^{1}H NMR ($CDCl_3$, 300 MHz), δ: 8.00, 7.67, 7.45, 7.25, 7.10, 6.97, 6.94, 6.75 (8 × d, 8H, ArH), 4.32, 4.02 (2 × m, 4H, OCH_2), 3.11, 2.69 (2 × s, 6H, NCH_3), 1.75 (m, 2H, OCH_2CH_2), 1.45−1.15 (m, 6H, $C_3H_6CH_3$), 0.89 (m, 6H, CH_3). ^{13}C NMR ($CDCl_3$, 75 MHz), δ: 165.8, 165.3, 160.9, 142.1, 141.6, 134.6, 132.6, 132.0, 130.2, 129.0, 128.0, 127.8, 127.5, 114.6, 68.0, 61.1, 60.5, 43.6, 43.1, 31.8, 31.4, 29.6, 29.3, 29.0, 25.6, 23.5, 22.5, 14.2, 13.9. MS (FD, 8kV), *m*/*z*: 420.2 (M^+). IR [cm^{-1}], ν: 2960, 2931, 2872, 2186, 1714, 1606, 1507, 1466, 1420, 1274, 1179, 738. UV−vis ($CHCl_3$): λ_{max}, nm (ϵ_{max}, L/(mol cm)) = 367 (14 900). Anal. Calcd for $C_{26}H_{32}N_2O_3$ (420.5): C, 74.26; H, 7.67; N, 6.38. Found: C, 74.52; H, 7.88; N, 6.38.

2.1.10. Stilbene 1b. Stilbene **1b** was prepared from 4-(cyanomethyl)benzoic acid ethyl ester (**6a**) (500 mg, 2.64 mmol), sodium hydride (133 mg, 5.28 mmol), and 4-hexyloxydibutyl-[(methylthio)phenylmethylene]ammonium iodide (**10b**) (1.298 g, 2.64 mmol) in the manner described in the general procedure. Yield: 612 mg (46%). ^{1}H NMR ($CDCl_3$, 300 MHz), δ: 8.02, 7.69, 7.43, 7.37, 7.12, 6.98, 6.96, 6.75 (8 × d, 8H, ArH), 4.31, 3.92 (2 × m, 4H, OCH_2), 3.43, 2.93 (2 × t, 4H, NCH_2), 1.81−1.11 (m, 16H, $NCH_2CH_2CH_2$, $C_4H_8CH_3$), 0.94−0.89 (m, 12H, CH_3). ^{13}C NMR ($CDCl_3$, 75 MHz), δ: 166.5, 165.3, 162.7, 161.3, 142.2, 141.8, 132.8, 131.9, 131.5, 129.5, 129.0, 128.3, 127.7, 127.4, 126.1, 121.5, 114.7, 84.1, 68.1, 60.9, 51.9, 51.4,-31.6, 30.1, 29.1, 25.7, 22.6, 19.9, 14.4, 14.0, 13.7. MS (FD, 8kV), *m*/*z*: 504.1 (M^+). IR[cm^{-1}] ν: 2959, 2927, 2871, 2187, 1714, 1603, 1507, 1466, 1420, 1273, 1178, 1103, 1018, 773. UV−vis ($CHCl_3$): λ_{max}, nm (ϵ_{max}, L/(mol cm)) = 377 (18 100). Anal. Calcd for $C_{32}H_{44}N_2O_3$ (504.7): C, 76.15; H, 8.79; N, 5.55. Found: C, 76.31; H, 8.85; N, 5.36.

2.1.11. Successive Buildup of Oligomers 2a,b and 3a,b. (For the general procedure, see Scheme 6.) The following reactions were performed under argon atmosphere in dry solvents. First, 4-cyanomethyl-4′-*N*,*N*-dibutylthioamidylbiphenyl[21] (**11b**) (1.0 g, 2.74 mmol) was dissolved in DMF (10 mL) and cooled to 233 K. Sodium hydride (95% w/w dispersion in mineral oil) (139 mg, 5.49 mmol) and 4-hexyloxydibutyl-[(methylthio)phenylmethylene]ammonium iodide (**10b**) (1.347 g, 2.74 mmol) were added, and after 6 h the solution was warmed to room temperature. The solvent was removed under vacuum and dichloromethane (8 mL) and trimethyloxonium tetrafluoroborate (448 mg, 3.02 mmol) were added to the brownish residue of thioamide **12b**. After 24 h the solvent was removed and one-half of the resulting ammonium salt **13b** (1.070 g, 1.37 mmol) was added to a solution of **6b** (298 mg, 1.37 mmol) and sodium hydride (95% w/w dispersion in mineral oil) (70 mg, 2.75 mmol) at 233 K in DMF (7 mL). After a reaction time of 6 h the mixture was warmed to room temperature and oligomer **2b** was obtained as a brownish oil, which was purified by chromatography on silica gel with an eluent mixture of ethyl acetate/petroleum ether of 1:2. The glassy, yellow product **2b** was obtained in 37% yield (237 mg).

For the preparation of oligomer **3b**, ammonium salt **13b** (1.070 g,1.37 mmol) was added to a solution of **11b** (500 mg, 1.37 mmol) and sodium hydride (95%) (70 mg, 23.0 mmol) at 233 K in DMF (15 mL). After 6 h and warming to room temperature, the solvent was distilled, and trimethyloxonium tetrafluoroborate (224 mg, 1.51 mmol) in dichloromethane (10 mL) was added to the residue to give the ammonium salt **14b**. Coupling with **6b** was performed analogously to the synthesis of **2b** (with **6b** (298 mg, 1.37 mmol) and sodium hydride (70 mg, 2.75 mmol)) to give the donor and acceptor substituted oligomer **3b**. This was also purified by chromatography on silica gel with an eluent mixture of ethyl acetate/petroleum ether 1:5 and the glassy, yellow product **3b** was isolated in 16% yield (260 mg).

2b. ^{1}H NMR ($CDCl_3$, 300 MHz), δ: 7.98−6.67 (16H, m, ArH), 4.29−3.84 (m, 4H, OCH_2), 3.32, 2.87 (2 × m, 8H, $N-CH_2$), 1.79−0.70 (m, 46H, alkyl-H). ^{13}C NMR ($CDCl_3$, 75 MHz), δ: 166.4, 164.2, 163.0, 160.6, 142.4, 136.9, 132.8, 131.9, 129.5, 129.0, 128.7, 128.4, 127.8, 126.9, 126.7, 126.5, 114.5, 86.0, 68.1, 60.4, 51.6, 51.4, 51.2, 31.5, 30.7, 25.7, 22.5, 21.0, 19.9, 19.2, 14.1, 14.0, 13.8. MS (FD, 8kV) *m*/*z*: 1192.9 (M^+). IR [cm^{-1}], ν: 2957, 2930, 2871, 2187, 1714, 1605, 1527, 1509, 1275, 1178, 1106, 773. UV−vis ($CHCl_3$): λ_{max}, nm (ϵ_{max}, L/(mol cm)) = 372 (25 500). Anal. Calcd for $C_{57}H_{74}N_4O_3$ (863.2): C, 79.31; H, 8.64; N 6.49. Found: C, 79.40; H, 8.80; N, 6.29.

3b. ^{1}H NMR ($CDCl_3$, 300 MHz), δ: 8.06−6,74 (m, 24H, ArH), 4.35−3.92 (m, 4H, OCH_2), 3.42, 2.93 (2 × m, 12H, $N-CH_2$), 1.85−0.66 (m, 60H, alkyl-H). ^{13}C NMR ($CDCl_3$, 75 MHz), δ: 166.1, 164.0, 163.1, 160.6, 141.4, 137.1, 132.8, 131.8, 129.4, 129.1. 129.0, 128.7, 127.9, 127.6, 127.0, 126.7, 126.6, 115.0, 68.8, 68.1, 60.4, 51.6, 51.4, 31.5, 30.2, 29.7, 25.0, 24.6, 22.5, 21.0, 19.9, 19.2, 14.9, 14.1, 14.0, 13.8. MS (FD, 8kV) *m*/*z*: 1192.9 (M^+). IR [cm^{-1}], ν: 2957, 2927, 2871, 2858, 2360, 2341, 2187, 1714, 1605, 1528, 1508, 1275, 1119, 749. UV−vis ($CHCl_3$): λ_{max}, nm (ϵ_{max}, L/(mol cm)) = 378 (35 500). Anal. Calcd for $C_{80}H_{100}N_6O_3$ (1193.7): C, 80.49; H, 8.44; N, 7.04. Found: C, 80.40; H, 8.45; N, 6.89.

The successive buildup of oligomers **2a** and **3a** was conducted analogously to the preparation of oligomers **2b** and **3b** using compounds **10a**, **11a**, and **6b**. **2a** and **3a** were obtained in 45 and 20% yields, respectively.

2a. ^{1}H NMR ($CDCl_3$, 300 MHz), δ: 7.99−6.70 (16H, m, ArH), 4.30−3.80 (m, 4H, OCH_2), 3.09, 2.62 (2 × m, 12H, $N-CH_3$), 1.75−1.52, 1.41−1.17, 0.93−0.72 (3 × m, 14H, alkyl-H). ^{13}C NMR ($CDCl_3$, 75 MHz), δ: 166.3, 164.1, 161.2, 141.7, 132.5, 131.5, 130.8, 129.3, 128.9, 128.5, 128.2, 127.6, 125.8, 126.5,

114.4, 67.9, 64.4, 43.7, 43.1, 42.9, 31.4, 30.6, 28.9, 25.5, 22.4, 19.1, 18.8, 13.6. MS (FD, 8kV), *m*/*z*: 694.5 (M^+). IR [cm^{-1}], ν: 2959, 2932, 2872, 2187, 1714, 1605, 1507, 1466, 1275, 1179, 1107, 738. UV−vis ($CHCl_3$): λ_{max}, nm (ϵ_{max}, L/(mol cm)) = 373 (28000). Anal. Calcd for $C_{45}H_{50}N_4O_3$ (694.9): C, 77.78; H, 7.25; N, 8.06. Found: C, 77.85; H, 7.34; N, 7.90.

3a. ^{1}H NMR ($CDCl_3$, 300 MHz), δ: 8.15−6.90 (m, 24H, ArH), 4.49−4.03 (m, 4H, OCH_2), 3.29, 2.86 (2 × m, 18H, N−CH_3), 1.98−1.00 (m, 18H, alkyl-H). ^{13}C NMR ($CDCl_3$, 75 MHz), δ: 166.4, 163.2, 162.8, 162.5, 137.0, 132.7, 132.0, 131.7, 131.5, 129.4, 129.1, 128.7, 128.4, 127.9, 127.1, 126.9, 126.7, 126.2, 114.6, 68.1, 64.8, 60.3, 43.8, 43.5, 43.1, 43.0, 31.5, 30.8, 30.7, 29.1, 29.0, 26.0, 22.5, 21.0, 19.2, 14.1, 14.0, 13.7, 13.0. MS (FD, 8kV), *m*/*z*: 940.7 (M^+). IR [cm^{-1}], ν: 2956, 2931, 2360, 2342, 1707, 1641, 1603, 1540, 1395, 1276, 1106, 749. UV−vis ($CHCl_3$): λ_{max}, nm (ϵ_{max}, L/(mol cm)) = 373 (36 900). Anal. Calcd for $C_{62}H_{64}N_6O_3$ (941.2): C, 79.12; H, 6.85; N, 8.93. Found: C, 79.34; H, 6.92; N, 8.70.

2.2. Dielectric Measurements. Dipole moments have been determined by measuring the (static) dielectric constant ϵ at $T = 295$ K of the compound dissolved in toluene (spectroscopic grade) as a function of the weight fraction $w_2 < 0.05$. The solution was placed between two brass plates of 20 mm diameter and 50 μm spacing, and the capacitance is measured with a HP-4284A impedance analyzer at a frequency of $f =$ 100 kHz. The resulting data $\epsilon(w_2)$ are linear in w_2 and an extrapolation of $w_2 \rightarrow 0$ yields $\epsilon = 2.340 \pm 0.001$, in good agreement with $\epsilon_1 = 2.379$[27] for pure toluene. For sufficiently polar molecules the effective dipole moment μ can be obtained using the Guggenheim approximation[28]

$$\mu^2 = \frac{27\epsilon_0 kTM_2\nu_1}{N_A(\epsilon_1 + 2)^2}\left(\frac{\partial\epsilon}{\partial w_2} - \frac{\partial n^2}{\partial w_2}\right) \qquad (1)$$

This equation uses the values for the mole fraction, M, the molecular volume, ν, and the weight fraction, w, where the indices 1 and 2 refer to the solvent toluene and the solute under study, respectively. Changes in the refractive index n have been disregarded; i.e., we applied the realistic assumption $\partial n^2/\partial w_2 \approx 0$.

The matrix material polystryrene (PS) is characterized by an average molecular weight $M_w = 181\,000$ and dispersity $M_w/M_n = 1.03$. The oligomer-doped PS films were cast onto the plate of a disk capacitor from a toluene solution and then carefully dried. The resulting typical film thickness was around 50 μm. The dielectric relaxation data $\epsilon^*(\omega)$ have been measured for frequencies $f = 2\pi\omega$ in the range 10^{-2} Hz $\leq f \leq 10^6$ Hz using a frequency response analyzer, Solartron SI-1260, equipped with a transimpedance amplifier, Mestec DM-1360. Sample temperatures were controlled by a N_2 gas stream which is thermally stabilized by a Novocontrol Quatro system. From the resulting impedance data we calculate the dielectric function $\epsilon^*(\omega) = \epsilon'(\omega) - i\epsilon''(\omega)$. The static dielectric constant $\epsilon_s = \epsilon'(\omega \rightarrow 0)$ can be inferred from the permittivity data $\epsilon'(\omega)$, whereas the characteristic time constant for dielectric relaxation is derived from the loss curves $\epsilon''(\omega)$. To this end the dielectric loss $\epsilon''(\omega)$ was subject to a fit according to the empirical function advanced by Havriliak and Negami[29] (HN)

$$\epsilon^*(\omega) = \epsilon'(\omega) - i\epsilon''(\omega) = \epsilon_\infty + \frac{\epsilon_s - \epsilon_\infty}{[1 + (i\omega\tau_{HN})^\alpha]^\gamma} \qquad (2)$$

where $\epsilon_\infty \approx n^2$ and ϵ_s are the high- and low-frequency limits of the permittivity $\epsilon'(\omega)$, respectively. The relaxation time is characterized by the value τ_{HN}, and the symmetric and asymmetric broadening of the loss curves are quantified by $0 < \alpha \leq 1$ and $0 < \alpha\gamma \leq 1$.

To obtain the dipole moments of the oligomers in the PS matrix, we infer the ϵ_s value for the 5% oligomer in PS film and ϵ_s determined for the pure PS, where both values have to be taken above T_g. The slope $\partial\epsilon^2/\partial w_2$ resulting from these two points, $w_2 = 0$ and $w_2 = 0.05$, then enters the Guggenheim eq 1 as for the toluene data.

Table 1. Dipole Moments μ (debye) for the Series of Compounds of Scheme 1 in Toluene (μ_{Tol}) and in Polystyrene (μ_{PS})[a]

compound	*N*	R	μ_{tol}	$\mu_{tol}/\sqrt{N}$	μ_{PS}	$\mu_{PS}/\sqrt{N}$	T_g/°C
1a	1	Me	5.08	5.08	4.66	4.66	91.5
2a	2	Me	6.28	4.44	5.31	3.75	98.4
3a	3	Me	5.64	3.25	5.28	3.05	95.9
1b	1	Bu	5.72	5.72	4.76	4.76	92.0
2b	2	Bu	7.43	5.25	6.61	4.67	97.3
3b	3	Bu	8.03	4.64	7.25	4.19	94.1
4b	2*n*	Bu	7.68	5.43	5.86	4.14	102.3
5[22]	1	Bu	6.12	6.12			
14[22]	2	Bu	7.10	5.02			
15[22]	3	Bu	7.91	4.57			

[a] Values are stated as a function of the number N of repeat units ($2n$ dipoles per n units in the case of the polymer **4b**) and for two different alkyl side chains, methyl (R = Me) and butyl (R = Bu). The compounds **5**, **14**, and **15** (analogous oligomers with biphenylene spacers and phenyl terminal groups) refer to ref 22. Values of T_g refer to DSC traces recorded at a heating rate of 5 K/min for the PS samples doped with the compound at a 5% level.

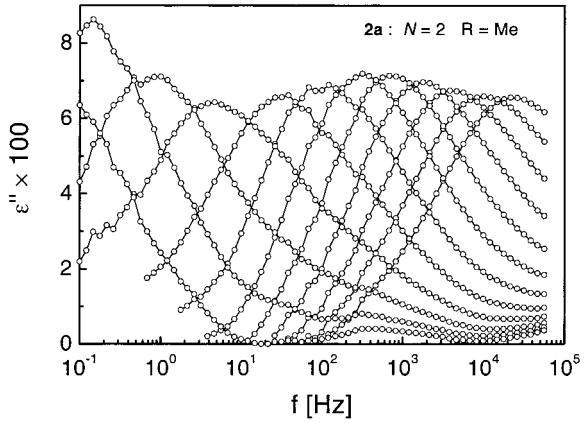

Figure 1. Dielectric loss spectra $\epsilon''(\omega)$ for a PS matrix doped with compound **2a** ($N = 2$, R = Me) at the 5% level by weight. The curves are parametric in temperature ranging from 372 to 416 K in steps of 4 K, in the order from low to high peak frequency.

3. Experimental Results

The experimentally obtained dipole moments μ for the series of oligomers in toluene and in PS are compiled in Table 1 as a function of the number of repeat units N and for the two different alkyl side groups, methyl and butyl. Note that the data for μ refer to the oligomer molecule as a whole, and not to the individual dipoles. The data set also includes values for $\mu/\sqrt{N}$ and μ/N for reasons which will be explained below.

Dielectric loss spectra in the frequency range 10^{-2} Hz $\leq f \leq 10^6$ Hz have been measured for the entire series of different oligomers shown in Scheme 1 dissolved at the 5% concentration level in PS. Figure 1 displays dielectric loss measurements of doped PS films parametric in temperature for the compound **2a** ($N = 2$ and R = CH_3), with the qualitative features of these curves being representative for all methyl substituted (R = CH_3) oligomers. Figure 2 shows the analogous data for the sample **2b** ($N = 2$ and R = C_4H_9), again representing the qualitative behavior of the other butyl-substituted (R = C_4H_9) oligomers. The striking difference seen here as regards the cases methyl vs butyl side chains is the appearance of a minor secondary peak for the methyl

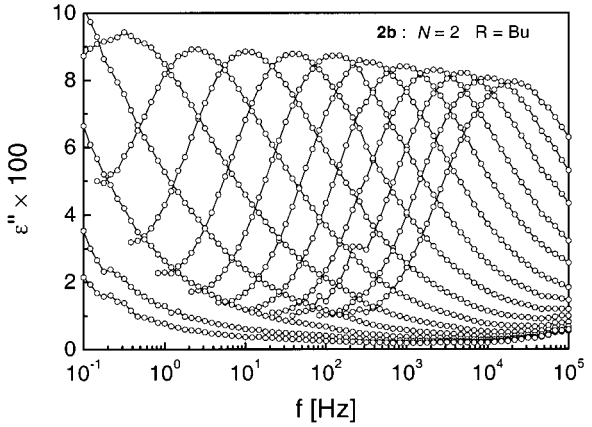

Figure 2. Dielectric loss spectra $\epsilon''(\omega)$ for a PS matrix doped with compound **2b** ($N = 2$, R = Bu) at the 5% level by weight. The curves are parametric in temperature ranging from 360 to 416 K in steps of 4 K, in the order from low to high peak frequency.

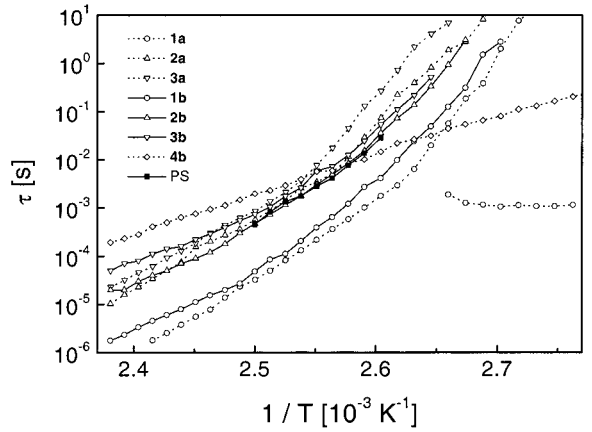

Figure 3. Plot of the characteristic time scales of dielectric relaxation, log(τ) vs $1/T$, for the various compounds (as designated) in the PS matrix at a concentration of 5 wt %. The data associated with pure PS are drawn as solid squares. The practically horizontal set of data refers to a secondary process of **1a**. The data of **4b** (open diamonds) represent an Arrhenius such as temperature dependence, whereas all other main processes display a VFT-like curvature in this plot.

case (**1a**, **2a**, **3a**), which is absent in butyl counterparts (**1b**, **2b**, **3b**). The different trends in the peak amplitude of the loss ϵ'' with temperature is a consequence of the secondary peak, which increases in amplitude toward higher temperatues, until it eventually appears to merge into the slower main peak.

The results concerning the characteristic relaxation times $\tau(T)$ are compiled graphically in Figure 3, scaled as $-\log(\tau/\mathrm{s})$ vs $1/T$. In the case of the oligomer/PS films the entire dielectric signals are governed by the polar donor/acceptor (DA) groups, whose dipole moments exceed that of the styrene segments significantly. Therefore, the relaxation times obtained for the doped PS films directly reflect the time scales of orientational mobility of the guest dipoles. The solid symbols in Figure 3 designate the dielectric relaxation times for the pure PS film, thereby outlining the segmental dynamics inherent in the PS matrix material.

4. Discussion

The dipole moments per molecule of the oligomers **1a**−**3b** and those per repeat unit of the polymeric compound **4b** attain values ranging from 5 to 8 D, where

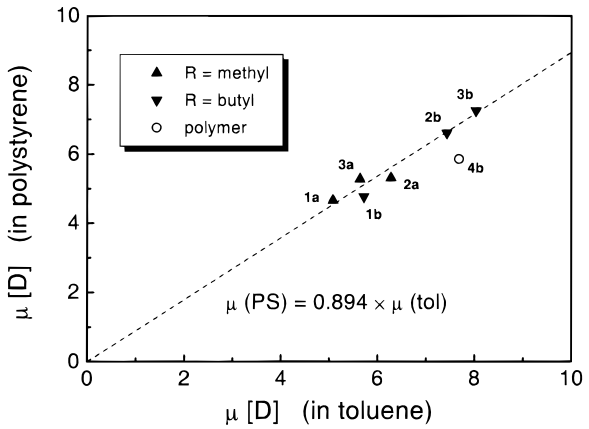

Figure 4. Relation between experimentally determined molecular dipole moments μ in fluid solution (μ_{tol}) and those in the polymer matrix (μ_{PS}) for the present series of compounds as labeled. A linear regression of the form $\mu_{PS} = a + b\mu_{tol}$ concerning the solid symbols leads to $a = -0.06$ and $b = 0.896$ with a correlation coefficient $R = 0.974$. This linear fit is plotted as dotted line.

$\mu \approx 5$ D is a typical value for donor/acceptor-substituted stilbenes. The concomitant slopes $\partial\epsilon/\partial w_2$ for the oligomers in toluene are concentration invariant up to $w_2 = 5\%$, which means that aggregation effects remain negligible in this range. The contribution of the terminal groups of the oligomers, hexyloxy ($C_6H_{13}O$) or butoxycarbonyl ($COOC_4H_9$), to the observed dipole moments is small, because the phenyl-terminated counterparts[22] to the structures **1b**, **2b**, and **3b** display very similar values for μ, namely 6.12, 7.10, and 7.91 D, respectively. Figure 4 emphasizes that the dipole moments obtained in the polymer matrix are consistent with those derived from the toluene solution results.

Our first interest is aimed at the relative orientation and motional degree of freedom of the individual dipoles (DA pairs) within the oligomer in toluene solution. We observe in Table 1 that the molecular dipole moment increases with the number N of DA pairs in the oligomer, indicating that the spacing between adjacent DA units is sufficient to suppress the tendency of antiparallel dipole alignment which would lead to decreasing values of $\mu(N)$. A rough inspection of the data in Table 1 also shows that the proportionality $\mu \propto N$ does not hold. Such a constant ratio μ/N, i.e., additivity of the dipole moment per repeat unit, may be expected only in the case of a strictly parallel dipole alignment within a molecule and in the absence of mutual degrees of freedom. This situation should not be realized because the rotational barriers are well below kT.

A further approach toward the understanding of $\mu(N)$ is to assume complete independence of the DA pairs as regards their orientation. Under this premise, a change in N is equivalent to a change in dipole concentration, leading to the dependence $\mu^2 \propto N$ or, equivalently, to a constant term $\mu/\sqrt{N}$. Experimental values for $\mu/\sqrt{N}$ are included in Table 1, indicative of a falling tendency as N increases, because μ is raised by an average factor of 1.3 only as N changes from 1 to 3. A more realistic calculation has to take account of the fact that the orientational degree of freedom of DA pairs or triples is confined to the rotation about the common long molecular axis and that mutual dipole interactions might play a role.

To rationalize the measured dipole moments in terms of a simple model for the rotational mobility, we conduct

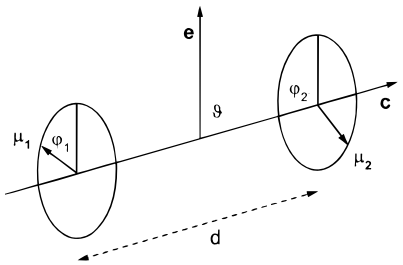

Figure 5. Schematic model of interconnected dipoles ($N = 2$, dimer) used in the calculation of effective dipole moments.

the following calculation. The molecule is modeled by its long axis, on which the appropriate number N of dipoles with moment μ is arranged with a fixed spacing d between adjacent dipoles. The dipoles are confined to orientations perpendicular to the long molecular axis. A schematic picture of this model for $N = 2$ is shown in Figure 5. The angles of free rotation of the two dipoles are φ_1 and φ_2. The connecting rigid axis c forms the angle ϑ relative to the direction e of the electric field E. Then, the projection factors of the two dipoles on the direction of the electric field are given by $\cos \theta_i = \cos \varphi_i \sin \vartheta$ ($i = 1, 2$). The total interaction energy W is given by $W = W_1 + W_2 + W_{12}$ with $W_i = -\mu_i E f \cos \theta_i$ ($i = 1, 2$) quantifying the interaction of the individual dipoles with the local field $E \cdot f$, where f represents an Onsager-type local field factor.[30] The remaining mutual interaction between two dipoles separated by a distance d is

$$W_{12} = \frac{\mu_1 \mu_2 \cos(\varphi_2 - \varphi_1)}{4\pi\epsilon\epsilon_0 d^3} \qquad (3)$$

Note that we assume a strict perpendicular alignment of the dipoles with respect to c, and therefore, the second term in the dipole−dipole interaction energy equation vanishes.

Using these definitions the following order parameters can be calculated: The average projection factors $\langle \cos \theta_i \rangle$ of the two dipoles with respect to e

$$\langle \cos \theta_i \rangle = \frac{\int_0^{\pi} \sin \vartheta \, d\vartheta \int_0^{2\pi} d\varphi_1 \int_0^{2\pi} d\varphi_2 \cos \theta_i e^{-W/kT}}{\int_0^{\pi} \sin \vartheta \, d\vartheta \int_0^{2\pi} d\varphi_1 \int_0^{2\pi} d\varphi_2 e^{-W/kT}}, \quad i = 1, 2 \qquad (4)$$

and the dipolar order parameter $\langle P_2 \rangle = {}^1/_2(3\langle \cos^2 \vartheta \rangle - 1)$ of the connecting axis, which is a measure for the electric field induced distortion of the otherwise isotropic orientational distribution of c

$$\langle P_2 \rangle = \frac{\int_0^{\pi} \sin \vartheta \, d\vartheta \int_0^{2\pi} d\varphi_1 \int_0^{2\pi} d\varphi_2 \frac{1}{2}(3 \cos^2 \vartheta - 1) e^{-W/kT}}{\int_0^{\pi} \sin \vartheta \, d\vartheta \int_0^{2\pi} d\varphi_1 \int_0^{2\pi} d\varphi_2 e^{-W/kT}} \qquad (5)$$

For the calculation of the average projection terms, the Boltzmann factor is expanded up to the second order

$$e^{-W/kT} \cong 1 - \frac{W}{kT} + \frac{1}{2}\left(\frac{W}{kT}\right)^2 \qquad (6)$$

While only the first-order expansion is often used to estimate the polar order in conventional poled polymer materials, dipole−dipole coupling is only included in the averaged terms by using the second and higher orders.

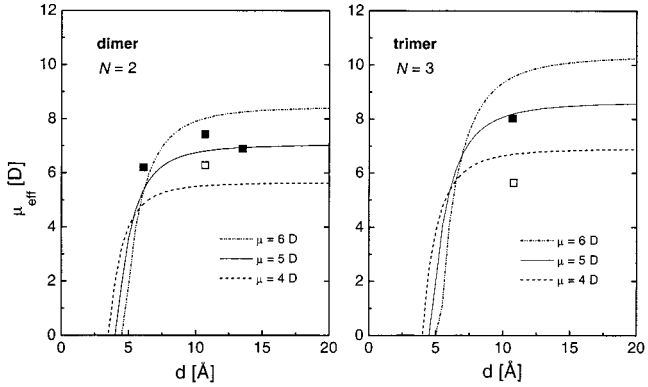

Figure 6. Effective dipole moment μ_{eff} in the low-field limit as a function of the distance d along the connecting axis for the dimer ($N = 2$) and trimer ($N = 3$), as obtained from the numerical integration of eq 4. The results are shown for dipole moment values of $\mu = 4$, 5, and 6 D, as indicated. The symbols represent the experimental μ_{tol} results from Table 1 for the compounds with R = Bu (■) and R = Me (□). The d values for the molecules are based on AM1 calculations.[31]

Finally, the effective dipole moment μ in the dielectric experiments is defined by

$$\mu_1 \langle \cos \theta_1 \rangle + \mu_2 \langle \cos \theta_2 \rangle = \mu \langle \cos \theta \rangle = \mu \frac{\mu E f}{3kT} \qquad (7)$$

which is based on the first-order approximation of the effective projection term $\langle \cos \theta \rangle = \mu E f / 3kT$, which is linear in the electric field E.

Since the component of the effective dipole moment perpendicular to the molecular axis is initially unknown, calculations have been performed for different values of $\mu_1 = \mu_2$. In the following, we will refer to the number N of dipoles per molecule in terms of the notation: monomer ($N = 1$), dimer ($N = 2$), and trimer ($N = 3$), irrespective of the remaining chemical constitution. For the trimer, all three dipole−dipole interaction terms were regarded, and the Boltzmann factor was again expanded up to the second order.

The results obtained by numerical integration of eqs 4 and 5 (the program Mathematica was used) are summarized in Figure 6. Dipole-dipole distances were determined by AM1 calculations[31] to be $d = 10.7$ Å for the biphenylene spacer used in compounds **1a**−**3b**. Also shown are data for dimers with R = Bu and either a phenyl spacer ($d = 6.1$ Å) or a tolane spacer ($d = 13.5$ Å).[32] According to the calculation the effective dipole moment is reduced due to dipole−dipole coupling for distances d smaller than approximately 10 Å and then levels off at a value of $N^{1/2}\mu_i$. The comparison between the calculated $\mu(d)$ values and the experimental data for the dimer and trimer shows a satisfactory agreement for the butyl-substituted components if the dipole moment per repeat unit is set to approximately 5 D. For R = Me, the results are less consistent, and the trimer shows a smaller μ relative to the dimer. Note that the calculation is based on a free rotation of the dipoles around the connecting axis, and it does not permit a significant component of the dipole moment parallel to the connecting axis. The good agreement between the calculated and the observed dipole moments suggests that the above model of a sequence of equidistant dipoles which are relatively free to rotate in a plane perpendicular to the long molecular axis is appropriate for characterizing the orientational behavior of the oligomers in an external electric field.

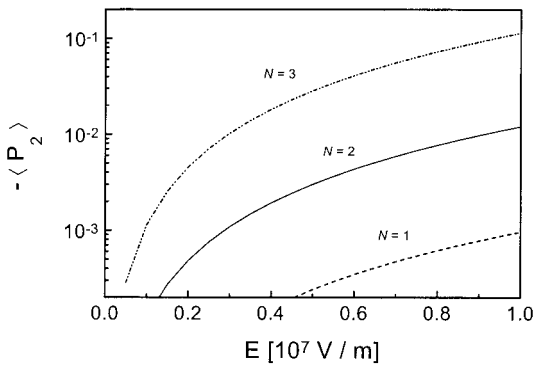

Figure 7. Calculated dipolar order parameter $\langle P_2 \rangle$, obtained by numerical integration of eq 5 as a function of the electric field E for the monomer ($N = 1$), dimer ($N = 2$), and trimer ($N = 3$) as designated. A dipole moment value $\mu_i = 5$ D per repeat unit and a distance $d = 10.7$ Å was assumed.

Even though the effective dipole moments are similar for the dimer and trimer for $d \leq 10$ Å, there is a large difference in the dipolar order parameter $\langle P_2 \rangle$, which is plotted as a function of the electric field E for the monomer, dimer, and trimer in Figure 7. Adding an additional dipole to the chain increases $\langle P_2 \rangle$ by almost 1 order of magnitude.

With respect to the relaxation of the dipoles two conclusions can be drawn. For a fixed orientation of the molecular axis c, the dipole−dipole distance in the oligomers is sufficiently large, such that their electrostatic coupling does not impede mutual reorientation. Accordingly, no signs of a preferred antiparallel orientation are observed. However, due to the constraints imposed by the rigid connection, the dipoles in one molecule cannot relax independently. Therefore, the bulkiness or size of the relaxing dipolar entity is larger for a system of sterically coupled dipoles (dimer or trimer), because the rotational motion of the molecular axis c is involved. The deviation from the isotropic distribution of the connecting axis c is significant for the dimer and trimer in the equilibrium state in the presence of an external electric field. In contrast to small isolated dye molecules, relaxation of the polar order of our oligomers thus requires rotation of a larger entity, which leads to a more pronounced coupling of the polar order to the segmental motion of the matrix. With regard to the temporal stability of polar order, a favorable consequence of the stronger coupling of the chromophore dynamics to the matrix is the longer persistence of dipole orientations as the material is cooled below T_g.

The relation between the dipole moments of the oligomers in toluene and in PS is highly systematic. Figure 4 is a graphic representation of the data compiled in Table 1 in terms of μ_{PS} vs μ_{tol}. A linear regression of the form $\mu_{PS} = c\mu_{tol}$ leads to $c = 0.894$. Therefore, the dipole moments in the highly viscous PS matrix are virtually identical to those obtained in fluid solution, irrespective of the number N of DA units and of the alkyl side groups R, methyl or butyl. We conclude that the average molecular conformations and configurations of the compounds under study are not altered significantly in the polymer matrix relative to the solution case. Especially, the degrees of freedom for mutual rotation of the DA units appear not to be suppressed by the PS matrix. Therefore, the effect of the viscous PS matrix reduces to governing the time scale of orientational dynamics, which is the concern of what follows.

Polystyrene is an amorphous polymer with a calorimetric glass transition temperature near $T_{g,cal} = 100$ °C and characterized by a low dielectric loss, due to the absence of large dipoles in the pure material.[33] For the investigation of the dynamics of polar guest molecules at moderate concentrations, the small dielectric relaxation strength of PS bears the advantage that the signals of the doped samples are unambiguously associated with the orientation of the dopant, whereas the matrix contributions are substantially smaller. However, the dipole moment of a PS segment is sufficient for measuring dielectric relaxation in order to assess the time scale of segmental motion as a function of temperature in the pure polymeric samples. The results for the dynamics of the pure matrix material are shown in Figure 3 by plotting τ logarithmically vs $1/T$ as solid squares. These experimental findings are compatible with the typical Williams−Landel−Ferry (WLF) or, equivalently, the Vogel−Fulcher−Tammann[34] (VFT) behavior of the structural relaxation in amorphous materials, where the latter reads

$$\tau(T) = \tau_0 \exp\left(\frac{B}{T - T_0}\right) \tag{8}$$

The relaxational behavior of guest molecules embedded in a polymer is a more complex issue. First, small molecules can act as plasticizer, thereby depressing the value of T_g for the sample. In terms of dielectric relaxation data, the glass transition can be outlined by the condition of $\tau_g = \tau(T_g) = 100$ s, which usually results in values comparable to the caloric $T_{g,cal}$ inferred from DSC experiments. The dynamic T_g estimated from Figure 3 depends on the oligomeric dopant but is not strongly correlated with the concomitant caloric data $T_{g,cal}$ determined for the series oligomer/PS samples. In particular, the relatively remote positions of the curves in Figure 3 associated with the monomers **1a** and **1b** are not paralleled by accordingly low values of $T_{g,cal}$. The extent to which a guest molecule is dynamically coupled to the segmental motion of the surrounding polymer is a matter of the dimensions of the guest relative to those of the host constituents. A systematic study of rotational guest/host dynamic coupling has revealed that a small guest tends to decouple and thus relax faster than the bulk material, whereas increasingly similar time scales are observed for larger guest molecules.[35] The orientational time scales for the compounds **1a**−**3b** follow this systematic trend, as seen in Figure 3. The two monomers **1a** and **1b** display orientational relaxation times which are a factor of ≈10 faster compared with the behavior of the pure PS matrix, a feature of dynamical decoupling which is observed in the entire experimental temperature range. The bulkier dimers, **2a** and **2b**, are associated with relaxation times which are close to the matrix values, and the trimers, **3a** and **3b**, are again somewhat slower. In agreement with the above conclusions drawn from the dipole moment studies, oligomers with more than one dipole are incapable of randomizing the dipolar alignment by independent rotations of the repeat units. Instead, the dimers and trimers require the concerted motion of 2 or 3 electrostatically coupled dipoles and the rotation of the long molecular axis for the destruction of their polar order. Accordingly, the demand in local free volume for such a motion will

significantly exceed that involved in the reorientation of isolated monomeric units, which are the only compounds associated with relaxation time scales faster than those of the structural relaxation of PS.

An unusual case with respect to the dynamical behavior is the polymeric guest material **4b**. Its temperature dependence $\tau(T)$ is no longer reminescent of the VFT-like curvature in the activation plot Figure 3. Instead, the dielectric relaxation time of this sample varies less with T and $\tau(T)$ is well approximated by the Arrhenius law $\tau = \tau_0 \exp(E_A/kT)$, albeit with a slight kink where this curve intercepts the $\tau(T)$ data for pure PS. A possible explanation of this pronounced decoupling from the matrix dynamics is a more folded structure, in which many of the guest repeat units are not in direct contact with the bulklike PS environment.

The effect of the alkyl substituent, methyl vs butyl, is 2-fold. The methyl substituted stilbene units (**1a**, **2a**, **3a**) display a secondary relaxation process whose signature in Figure 1 is an additional loss peak around $f = 10^3$ Hz, which is not observed for the corresponding butyl compounds (**1b**, **2b**, **3b**). Such dielectric secondary processes are usually associated with local librational motions of the dipoles, which persist also in the glassy state of the material.[33] The bulkier butyl group seems to frustrate this residual molecular motion due to higher steric demands. Second, the effective dipole moments of the butyl-substituted compounds are systematically higher than those found for the methyl counterparts, although the dipole moment of the stilbene unit should not be affected significantly.

5. Conclusions

We have studied the orientational behavior of a series of novel oligophenylenevinylenes which carry a sequence of hyperpolarizable and dipolar donor−acceptor pairs, designed to allow for a free rotation of the dipole orientation in a plane perpendicular to the long molecular axis. The effective dipole moments measured in toluene and polystyrene lead to the conclusion, that these oligomers are capable of increasing the concentration of hyperpolarizable chromophores without introducing drawbacks on the achievable polar order. For the present molecules with biphenylene spacers between DA pairs, the dipole−dipole separation $d \approx 10.7$ Å turns out to represent a good balance between a high chromophore density (small d) and small electrostatic interactions among adjacent dipoles. Both features are favorable as regards a high degree of polar order required for second-harmonic generation. The experimental dipole moments are consistent with those derived from electrostatical calculations based on a chainlike array of equidistant dipoles with $\mu = 5$ D, which are free to rotate in planes perpendicular to the connecting axis. For the oligomers, the dipole−dipole interaction within a molecule is governed by the sterical constraint of the common molecular axis, such that the reorientation of larger entities are involved for $N \geq 2$ relative to the monomer case. For the compounds with two and three DA pairs, **2a**,**b** and **3a**,**b**, we observe accordingly that the temporal persistence of polar order in the oligomer/polystyrene samples is limited only by the structural relaxation time of the polymeric matrix. The smaller molecules, **1a**,**b**, reorient faster than the polystyrene segments by a factor of ≈ 10. It is also observed that the butyl side group attached to the chromophore reduces librational motion of the dipoles relative to the methyl substituted systems.

Acknowledgment. Financial support by the Bundesministerium für Bildung und Forschung through the OPTIMAS project (No. 03N1021B7) and the Volkswagen-Photonik project (No. I-69820) and by BRITE-EURAM OSCA (BRPR-CT97-0469) is gratefully acknowledged.

References and Notes

(1) Singer, K. D.; Sohn, J. E.; Lalama, S. J. *Appl. Phys. Lett.* **1986**, *49*, 248.
(2) Bauer, S. *Appl. Phys. Rev.* **1996**, *80*, 5531.
(3) Prasad, P. N.; Williams, D. J. *Introduction to Nonlinear Optical Effects in Molecules and Polymers*; Wiley-Interscience: New York, 1991.
(4) Eich, M.; Bjorklund, G. C.; Yoon, D. Y. *Polym. Adv. Technol.* **1990**, *1*, 189.
(5) Walsh, C. A.; Burland, D. M.; Lee, V. Y.; Miller, R. D.; Smith, B. A.; Twieg, R. J.; Volksen, W. *Macromolecules* **1993**, *26*, 3720.
(6) Goodson, T.; Wang, C. H. *Macromolecules* **1993**, *26*, 1837.
(7) Hampsch, H. L.; Yang, J.; Wong, G. K.; Torkelson, J. M. *Macromolecules* **1990**, *23*, 3648.
(8) Schüssler, S.; Richert, R.; Bässler, H. *Macromolecules* **1994**, *27*, 4318.
(9) *Electrets*; Sessler, G. M., Ed.; Topics in Applied Physics 33; Springer: Berlin, 1987.
(10) *Nonlinear Optical Properties of Organic Molecules and Crystals*; Chemla, D. S., Zyss, J., Eds.; Academic Press: New York, 1987.
(11) Köhler, W.; Robello, D. R.; Dao, P. T.; Willand, C. S.; Williams, D. J. *J. Chem. Phys.* **1990**, *93*, 9157.
(12) Singer, K. D.; King, L. A. *J. Appl. Phys.* **1991**, *70*, 3251.
(13) Dhinojwala, A.; Wong, G. K.; Torkelson, J. M. *Macromolecules* **1993**, *26*, 5943.
(14) Guan, H. W.; Wang, C. H.; Gu, S. H. *J. Chem. Phys.* **1994**, *100*, 8454.
(15) Wegner, G.; Neher, D.; Heldmann, C.; Servay, T. K.; Winkelmann, H. J.; Schulze, M.; Kang, C. S. *Mater. Res. Soc. Symp. Proc.* **1994**, *328*, 15.
(16) Schüssler, S.; Richert, R.; Bässler, H. *Macromolecules* **1995**, *28*, 2429.
(17) Köhler, W.; Robello, D. R.; Willand, C. S.; Williams, D. J. *Macromolecules* **1991**, *24*, 4589.
(18) Blackburn, F. R.; Cicerone, M. T.; Ediger, M. D. *J. Polym. Sci., Part B: Polym. Phys.* **1994**, *32*, 2595.
(19) Pauley, M. A.; Guan, H. W.; Wang, C. H. *J. Chem. Phys.* **1996**, *104*, 6834.
(20) Schüssler, S.; Richert, R.; Bässler, H. *Macromolecules* **1996**, *29*, 1266.
(21) Klärner, G.; Former, C.; Martin, K.; Räder, J.; Müllen, K. *Macromolecules* **1998**, *31*, 3571.
(22) Klärner, G.; Former, C.; Yan, X.; Richert, R.; Müllen, K. *Adv. Mater.* **1996**, *8*, 932.
(23) Former, C.; Klärner, G.; Wagner, M.; Müllen, K. *J. Prakt. Chem.* **1998**, *340*, 367.
(24) Klärner, G.; Leuninger, J.; Former, C.; Soczka-Guth, T.; Müllen, K. *Macromol. Symp.* **1997**, *118*, 10.
(25) Snyder, H. R.; Merica, E. P.; Force, C. G.; White, E. G. *J. Am. Chem. Soc.* **1958**, *80*, 4622.
(26) Bayle, J.-P.; Bui, E.; Perez, F.; Courtieu, J. *J. Bull. Soc. Chim. Fr.* **1989**, *4*, 532.
(27) *Handbook of Chemistry and Physics*; Lide, D. R., Ed.; CRC: Boca Raton, FL, 1995.
(28) Riande, E.; Saiz, E. *Dipole Moments and Birefringence of Polymers*; Prentice Hall: Englewood Cliffs, NJ, 1992.
(29) Havriliak, S.; Negami, S. *J. Polym. Sci., Part C: Polym. Symp.* **1966**, *14*, 89.
(30) Böttcher, C. J. F. *Theory of Electric Polarization*; Elsevier: Amsterdam, 1973; Vol. I.
(31) Stewart, J. J. P. *J. Comput. Chem. 2* **1989**, *209*, 221.
(32) Former, C. Ph.D. Thesis, Mainz University, 1999.
(33) McCrum, N. G.; Read, B. E.; Williams, G. *Anelastic and Dielectric Effects in Polymeric Solids*; Wiley: New York, 1967.
(34) Vogel, H. *Phys. Z.* **1921**, *22*, 645. Fulcher, G. S. *J. Am. Ceram. Soc.* **1923**, *8*, 339.
(35) Inoue, T.; Cicerone, M. T.; Ediger, M. D. *Macromolecules* **1995**, *28*, 3425.

MA9902403